



Inductively coupled plasma nanoetching of atomic layer deposition alumina

Han, Anpan; Chang, Bingdong; Todeschini, Matteo; Le, Hoa Thanh; Tiddi, William; Keil, Matthias

Published in:
Microelectronic Engineering

Link to article, DOI:
[10.1016/j.mee.2018.02.023](https://doi.org/10.1016/j.mee.2018.02.023)

Publication date:
2018

Document Version
Peer reviewed version

[Link back to DTU Orbit](#)

Citation (APA):
Han, A., Chang, B., Todeschini, M., Le, H. T., Tiddi, W., & Keil, M. (2018). Inductively coupled plasma nanoetching of atomic layer deposition alumina. *Microelectronic Engineering*, 193, 28-33.
<https://doi.org/10.1016/j.mee.2018.02.023>

General rights

Copyright and moral rights for the publications made accessible in the public portal are retained by the authors and/or other copyright owners and it is a condition of accessing publications that users recognise and abide by the legal requirements associated with these rights.

- Users may download and print one copy of any publication from the public portal for the purpose of private study or research.
- You may not further distribute the material or use it for any profit-making activity or commercial gain
- You may freely distribute the URL identifying the publication in the public portal

If you believe that this document breaches copyright please contact us providing details, and we will remove access to the work immediately and investigate your claim.

Inductively coupled plasma nanoetching of atomic layer deposition alumina

Authors:

Anpan Han, Bingdong Chang, Matteo Todeschini, Hoa Thanh Le, William Tidli, Matthias Keil.

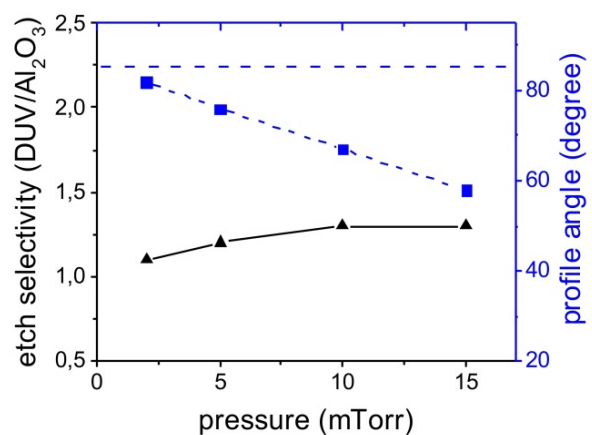
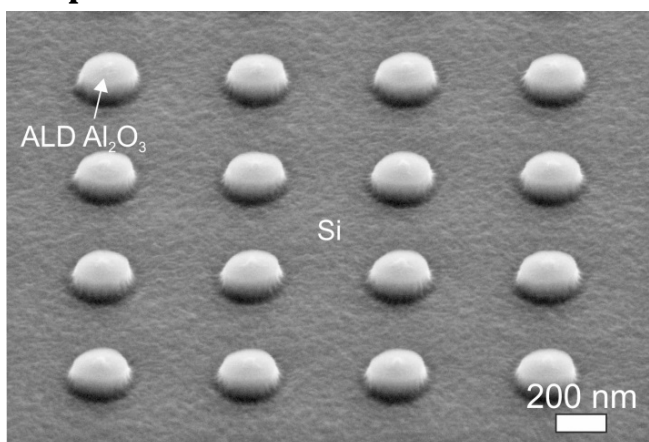
DTU Danchip CEN, Technical University of Denmark, Ørsteds Plads, Building 347, 2800 Kgs. Lyngby, Denmark.

Corresponding author: Anpan Han. Email: anph@dtu.dk

Abstract

Al_2O_3 thin-film deposited by atomic layer deposition is an attractive plasma etch mask for MEMS and NEMS. 20-nm-thick Al_2O_3 mask enables through silicon wafer plasma etching. Al_2O_3 is also an excellent etch mask for other important MEMS materials such as silicon dioxide, silicon nitride, and diamond. In this report, we systematically study nanoscale plasma etching of Al_2O_3 with electron beam lithography and deep UV resist masks. The gas composition and pressure were tuned for optimal etching, and redeposition conditions were mapped. With a BCl_3 and Ar plasma chemistry, the Al_2O_3 etch rate was controlled to between 0.1 to 1 nm/min. The etch selectivity of Al_2O_3 over resist ranged between 1:4 to 1:1. Etch-rate was linearly dependent on the substrate bias power. The etch profile angle can be controlled to between 20 and 82° that almost preserved the resist profile angle. For Al_2O_3 patterned with deep UV lithography, the smallest structures were 220 nm. For electron beam lithography patterns, the smallest gratings were 18-nm-wide with 50-nm-pitch. Using alumina as a hard mask, we show aspect ratio of 7-10 for subsequent silicon plasma etching, and we etched diamond nanopillars in single crystalline diamond. Based on these studies, we provide guidelines for alumina plasma etching on the nanoscale.

Graphical abstract



Keywords

Plasma etching, aluminum oxide, atomic layer deposition, inductively coupled plasma, electron beam lithography, deep UV lithography

Introduction

Amorphous Al_2O_3 thin-film deposited by atomic layer deposition (ALD) is an attractive plasma etch-mask for NEMS and MEMS. The etch selectivity of silicon over Al_2O_3 is outstanding [1] and can be as high as 100000:1 [2]. This is a remarkable improvement compared to 30:1 for photoresist. Al_2O_3 is also an excellent plasma etch mask for silicon nitride (57:1) [3], silicon dioxide (40:1) [3], and diamond which is normally etched by very powerful oxygen plasma using a silicon dioxide mask [4], [5]. In addition to etch deeper, compared to EBL and DUV resist masks, the main advantage of a thin hard mask is that the mask does not change during etching, and we can avoid undesired etching effects caused by mask erosion. Unlike polycrystalline ALD TiO_2 [6] which also has excellent selectivity, alumina is amorphous and preserve the original surface finish of the underlying substrate. Plasma etching of ALD Al_2O_3 [2], [7]–[12], and more detailed studies on plasma etching of sapphire exist [3], [13], [14]. Tegen and Moll studied plasma etching of sapphire using three plasma instruments including chemistry combinations of Ar, HCl, Cl_2 , HBr, CF_4 , SF_6 , CHF_3 , NF_3 [3]. They reported CF_4 plasma has the fastest etch rate of 1.2 nm/s. However, as the etch product AlF_3 is non-volatile, it is likely that the process is extremely physical. Hsu et al. reported BCl_3/Cl_2 chemistries, in agreement with Tegen and Moll, Cl_2 did not etch Al_2O_3 well, but 80% BCl_3 etched 10 times faster, and the etch rate is comparable to CF_4 plasma. This is because BO_xCl_y is volatile, while Cl alone does not form volatile compounds with oxygen. Complementary studies by Rasmussen showed Cl_2/BCl_3 plasma with 1.2 nm/s etch rate [15].

While previous studies optimize for highest etch rate, there are only two reports that optimize for etching with resist as etch mask. Rasmussen reported etch selectivity of UV photoresist over alumina can be as high as 2:1 using an inductively coupled plasma (ICP) [15]. Wang and Goryll showed selectivity of PMMA resist over alumina be 5:1 using a pure BCl_3 plasma and a reactive ion etching instrument [16]. ALD alumina can also assist nanopattern transfer of directed self-assembly of block co-polymers with great fidelity [17], [18]. We were not able to find systematic studies of nanoscale ICP etch of ALD alumina, which is important if alumina must be used as an etch mask in the nanoscale. In this study, using EBL and deep UV (DUV) nanopattern resist masks, we report a systematic study of nanoscale ICP etching of ALD alumina with a BCl_3 and Ar plasma chemistry. Having optimized ICP etching, we transferred nanopatterns of alumina into the underlying silicon substrate.

Materials and Methods.

ALD alumina coated silicon samples were either coated with EBL or DUV resist and subsequently patterned by either EBL [19] or DUV lithography. The resist patterns were then transferred into the alumina by ICP etching. The ALD alumina patterns were used as an etch mask for ICP etching of silicon. We describe the details in the below.

Using Picosun R200 ALD instrument, silicon wafers (100 mm diameter) were coated with 100 nm of alumina at 300 °C using tetra methyl aluminum and H_2O precursors. For each ALD reaction cycle, the precursor

pulse time was 0.1 s and the nitrogen purge flow was 150 sccm, the purge time was 4 s [20]. The final thin-film thickness was measured using spectroscopic ellipsometer (Vase, J.A. Woollam Co., Inc.).

For DUV lithography experiments, the alumina coated Si wafers were dehydrated and vapor primed with HMDS at 150 °C degrees using a 310TA-E system from YES Inc. All resist processing and development were done by two robot systems (Gamma 2M, Süss). The 65-nm-thick bottom antireflective coating (BARC, DUV42s-6 from Brewer Science) layer was spin-coated at 4700 rpm for 60 s and soft baked at 175 °C for 60 s. The 360-nm-thick DUV resist (KRF M230Y from JSR-Micro) was spin-coated at 2500 rpm for 60 s and soft baked at 130 °C for 90 s. Carefully designed test resist patterns were made using a Canon DUV stepper (FPA-3000EX4) equipped with a 248 nm KrF excimer laser light source. Gratings, pillar and cavity arrays with as small as 200 nm critical dimensions were patterned down to 400 nm pitch. For each individual pattern, both the exposure dose and the focus were optimized with the help of the ProLith™ simulation software from KLA-Tencor in order to achieve the largest depth of focus. In the simulations a rectangular shaped process window was used with a CD tolerance of $\pm 3\%$ and an exposure latitude of 1.5%. For the cavity, grating and pillar arrays, best doses was respectively 40.6, 20.1 and 14.7 mJ/cm² with focus offsets of respectively 0.15, 0,17 and 0,16 μm , measured from the top of the resist surfaces into the resist. The simulations for the cavity, grating and pillar arrays led to critical dimensions of respectively 207.8, 195.7 and 206.1 nm and the achieved depth of focuses were respectively 0.32, 0.86, and 0.36 μm . The samples were post exposure baked at 130 °C for 60 s and developed in AZ726 (AZ Electronic Materials) for 60 s, rinsed in DI water and dried by spin coating in a gentle nitrogen stream. The developer contains 2.38% TMAH that requires careful handling. The wafers were optically and SEM inspected. The BARC layer is not removed during development, and it was ICP (Pegasus, SPTS) etched with an oxygen chemistry. The parameters are 40 sccm O₂ flow, 5 mTorr pressure, 205 W coil power, and 20 W substrate bias power. The BARC etch rate was 2.0 nm/s.

For EBL, the ALD alumina coated Si wafers were dehydrated for 30 min at 250 °C in a convection oven. The EBL instrument is a JEOL JBX-9500FSZ with robot cassette sample loader installed in a specially designed cleanroom laboratory [19], the beam current was set to 0.2 nA for minimal beam diameter (4 nm). For positive-tone resist, we used CSAR 62 from AllResist Germany and ZEP520A from Zeonchemicals Japan. For 200-nm-thick CSAR resist coating, CSAR 62 was diluted 1:1 in anisole, spin coated at 4000 rpm for 30 s, and soft baked at 90 °C for 60 s. For 80-nm-thick ZEP resist coating, ZEP resist was diluted 1:1 in anisole, spin coated at 5000 rpm for 60 s, and soft baked at 180°C for 60 s. After EBL exposure, we developed for 60 s in AR-600-546. ZEP resist was exposed with dose 250 $\mu\text{C}/\text{cm}^2$, developed in ZED N50 for 60 s, and rinsed in IPA for 60 s. For negative-tone resist, we used hydrogen silsesquioxane (HSQ) XR-1541-002 resist from Dow Corning. It was spin coated at 6000 rpm for 60 s (acceleration rate 4000 rpm/s), and soft baked at 80 °C for 30 s. After spin coating, the resist thickness was 38 nm measured by ellipsometry. The exposure dose was 20 mC/cm². After exposure, it was developed in AZ 726 MIF (2.38% TMAH, with 4% NaCl) at room temperature for 20 s, and rinsed in DI water for 60 s. The ALD alumina is etched by the developer, the etch rate was measured to 3 nm/min. To remove HSQ resist residues, samples were immersed in 0.02% Hydrofluoric acid (HF) for 10 s.

For pattern transfer into ALD alumina we used an ICP instrument (ICP Plus SPTS). The substrate temperature was set to 20 °C, the platen and coil frequencies were set to 13,56 MHz, the chamber and lid heaters were set to respectively 45 and 50 °C. The gases were BCl₃, and Ar. The total gas flow rate was 30

sccm, and the coil power was set to 1200 W which are well-balanced parameters for our ICP instrument [15]. To rule out instrument day to day drift, experiments used to construct each graph were performed uninterrupted, and 10 min oxygen plasma preconditioned the plasma chamber between every data point. Details of the instrument and alumina etch stability can be found in the PhD thesis of Rasmussen [15].

For silicon etching, we used an ICP instrument (Pegasus, SPTS). For ZEP resist patterns, remaining ZEP resist was removed by oxygen plasma such only ALD alumina served as the etch mask. For HSQ resist, we did not remove the remaining resist as the remover also quickly etched ALD alumina. A continuous Si etching process was applied, with 80 sccm C_4F_8 , and 35 sccm SF_6 , the processing pressure was 15 mTorr, and substrate holder temperature was $-19\text{ }^\circ\text{C}$. The sample was fixed to the sample holder by electrostatic clamping and the backside of the sample was helium cooled. The coil power was 900 W and the platen power was 40 W. This silicon etch was known to generate nanograss in areas with only silicon exposed to the plasma. Patterns on ZEP resist were etched for 15 minutes, HSQ resist gratings were etched for 2 minutes, and HSQ resist pillars for 6 minutes.

For diamond patterning and etching, we coated single crystalline diamond samples with 10-nm-thin ALD alumina, which will serve as the hard mask for diamond ICP etching. For patterning on single crystalline diamond samples, we needed to use our organic ice resist (OIR) method [21], because we were not able to uniformly spin coat EBL resist on 2×2 mm square diamond samples. For the OIR patterning, 60 nm of nonane ice was condensed onto the cold diamond sample and exposed at 20 keV. After OIR sublimation, the alumina was etched. The alumina is then used as the hard mask to etch diamond with ICP (Plus, SPTS) using a pure oxygen plasma.

Results and discussions

We carefully designed experiments exploring and optimizing ICP etching of alumina. Our strategy to explore a multi-parameter etch process is to firstly investigate the intensive parameters and subsequently probe the extensive parameters. The intensive parameters such as plasma chemistry and pressure have the greatest and often qualitative impact on the etching process, while instrument dependent extensive parameters such as substrate bias play a minor and quantitative role.

Following this strategy, we firstly explored the gas chemistry and pressure. We selected an Ar and BCl_3 gas combination based on the following. Hsu et al. showed high etching rates of sapphire with a 80% BCl_3 and 20% Cl_2 plasma at 5 mTorr [13]. The addition of 20% Cl_2 increased the etch rate by 10 %. The added etch rate is not relevant for nanostructures, and hence we did not add Cl_2 to our plasma. Rasmussen etched sapphire using the same ICP instrument as in this study, and the best selectivity to resist was obtained at 0.5 mTorr, which was the lowest possible plasma pressure [15]. Despite the fast etch rate and good selectivity, unfortunately 0.5 mTorr plasma pressure was often unstable for our and most ICP instruments. Furthermore, 10 mTorr was required to strike the plasma, and the stabilization process might be sufficient to etch very thin layers of alumina. Kim and colleagues added Ar to the plasma [7]–[10], and this achieved a low partial pressure of reactive species and sustained a robust plasma. Unfortunately, how the addition of Ar affects the resist etching was not reported. While Wang and Goryll showed important result on nanoscale patterning of alumina, they used a RIE instrument which design is very different from ICP instruments.

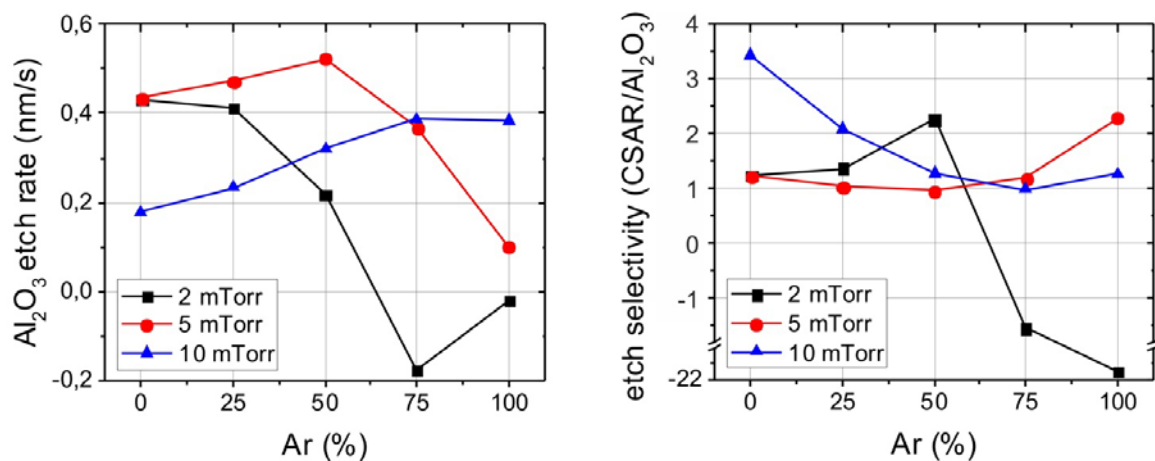


Figure 1. The influence of plasma chemistry and pressure on alumina etch rate and selectivity to the CSAR EBL resist. The plasma contained Ar and BCl₃ mixture. All other plasma parameters were kept constant.

Based on and inspired by the above prior art, we added Ar to BCl₃ and measured the CSAR EBL resist etch rate and etch selectivity over alumina (Fig. 1). The total pressure was between 2 and 10 mTorr, and the bias was fixed to 30 W. Results in figure 1 shows that at 2 mTorr, the etch rate decreased drastically with addition of Ar. Above 50% Ar, we observed redeposition which resulted in a thicker mask, a negative etch rate and negative selectivity. For 5 mtorr, the etch rate and selectivity peaked at 50% Ar. Etch rate at 5 mTorr was higher than at 10 mTorr, and the selectivity was comparable. For 10 mTorr, the etch rate increased with Ar, and at 75% Ar, the etch rate was twofold compared to pure BCl₃ plasma. The etch rate seemed to be very high at 100% Ar, but the resist mask was roughened, and we observed many particles on the sample that possibly originated from the Ar sputtering of reactor chamber. Our results show that 100% Ar process gave poor results, and 100% BCl₃ at 10 mTorr gave less good selectivity which was in agreement with previous study [16]. Depending on the pressure, the selectivity was up to 3.5 fold better than a pure BCl₃ plasma. Comparing all pressures and Ar content, the most robust (good selectivity, etch rate, and stable plasma) etching condition was between 5 and 10 mTorr, and about 50% Ar. According to these results, apparently, 5 mTorr, 50% Ar and BCl₃ mixture was best suited for etching alumina. Another important advantage, at 5 mTorr the plasma can be easily established without a high pressure plasma striking and prolonged stabilization step. The plasma striking process can be sufficient to etch very thin layers, and hence creating a critical error in the etching process.

Importantly, alumina etch longer than about 10 min caused redeposition. X-ray photoelectron spectroscopy measurements revealed the redeposit contained aluminum, carbon, oxygen, and chlorine. Redeposition was prevented by 10 min oxygen plasma conditioning of ICP chamber. We speculated that the carbon from the resist formed polymer like substances with the other elements, and it accumulated with time in the plasma chamber, and eventually caused redeposition as the substrate was kept at the lowest temperature in the plasma chamber. This C_wAl_xCl_yO_z polymer can and must be removed by oxygen plasma to avoid redeposition.

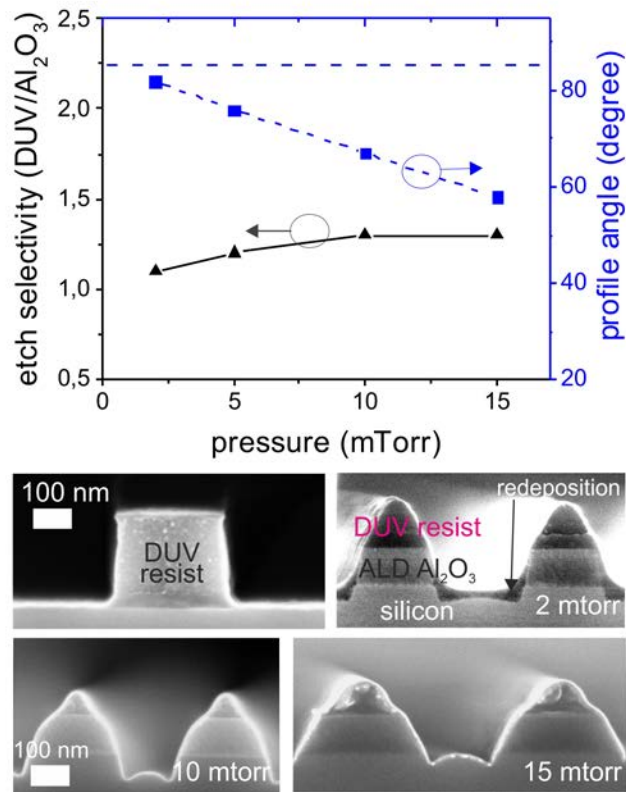


Figure 2. ICP pressure effects on the alumina etch profile angle and etch selectivity of DUV resist over alumina. The horizontal blue dashed line is the DUV resist profile angle. SEM cross-section images of DUV resist gratings before etching, after 2mTorr etch, 10 mTorr etch, and 15 mTorr etch. The remaining DUV resist was not removed before cleaving and SEM imaging. A thin layer of Au was sputter on top of the resist to avoid charging during SEM imaging.

Having found an apparent optimal plasma chemistry, we investigated the etch profile dependence on pressure. The etch profile is particularly important for nanoscale etching because an uncontrolled etch profile can remove nanopatterns completely. Figure 2 shows the etch profile angle of the etched alumina, and the etch selectivity of DUV resist over alumina. The etching pressures were between 2 and 15 mTorr. The etching gas contained 50% BCl₃ and 50% Ar. The substrate bias power was set to 30 W. We examined the DUV pattern cross-sections with SEM. The profile angle of DUV resist after lithography was 85°. After etching at all pressures, we observed severe mask erosion, the sharp corners of the resist mask were rounded. Mask erosion plays a minor role at low etching pressure, which agrees well with the better selectivity. It is highly likely that this mask erosion leads to lower etch profile angles. The alumina etch profile angle decreased with increasing pressure, from 82° at 2 mTorr to 58° at 15 mTorr. The selectivity slightly deteriorated with increasing pressure. Both effects were because at higher pressures the etching was more physical as Ar sputtering played a more important and dominant role. This might be counter intuitive because higher pressures normally lead to more isotropic profiles, but previous [7], [10] and our results (Figure 1) showed that BCl₃ etched poorly at high pressures, and this suggest at higher pressures Ar dominates the etching. At 2 mTorr, the etching was almost anisotropic and preserved the DUV resist profile. At 2 and 5 mtorr, when the alumina film was etched through, and the silicon was exposed to the plasma,

redeposition took place. It was unclear when the redeposition took place as we observed that the plasma etched the silicon too. XPS measurements showed that the redeposit contained mainly carbon, oxygen, chlorine, and boron. There were also traces of silicon and aluminum. We did not observe redeposition at 10 and 15 mTorr. We reasoned that the sputtering Ar removes the nonvolatile compound. Our results showed that the chemistry of the underlying substrate material is also important for an etching process. The over etching into the silicon caused trenching that was clearly visible in the cross-section SEM images in Figure 2. Two effects are known to cause trench formation; firstly, the non-uniformity of Ar ion flux density caused by the grating geometry may cause trenching [22], secondly, the local charging of the resist and alumina hard mask locally deflects ions and lead to trenching [23].

We did not investigate the effects of elevated substrate temperature as most resists decompose and selectivity deteriorates. For below ambient substrate temperatures, we reasoned that redeposition problems will become more severe, and the interested reader is referred to Yang et al. [11]. Having established the dominating intensive parameters, we then investigated the extensive parameters. They are the gas flow, coil power, and platen power. The gas flow and coil power together generates the density of reactive species and the ionization in the plasma. Their optimal magnitudes depend on the design of the ICP tool, e.g. reaction chamber volume, vacuum system, etc. The etch rate is typically linearly dependent on coil power [11]. For our ICP tool, 30 sccm total gas flow is optimal, and coil power is 80% of its maximum value. For optimization detail please refer to Rasmussen [15].

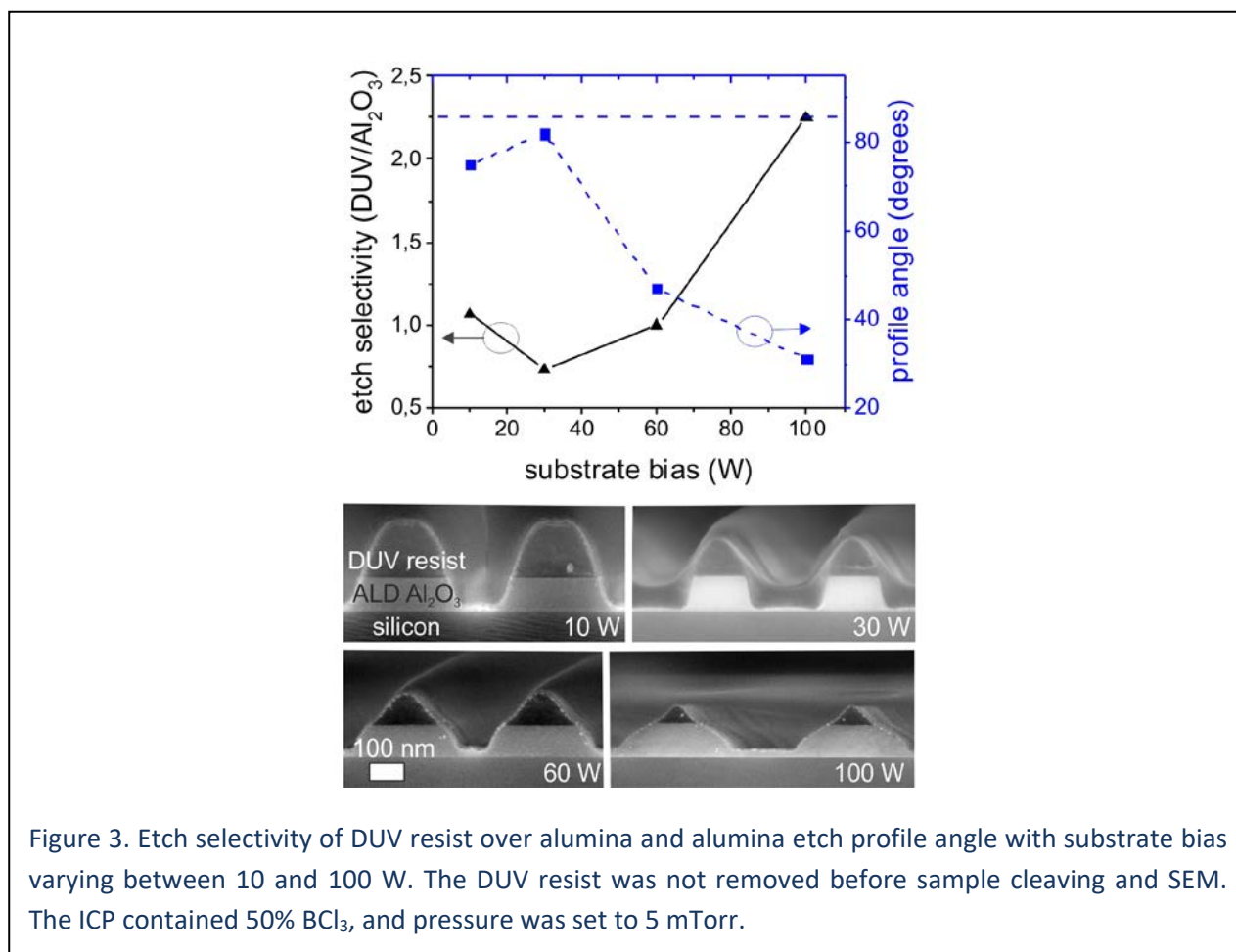
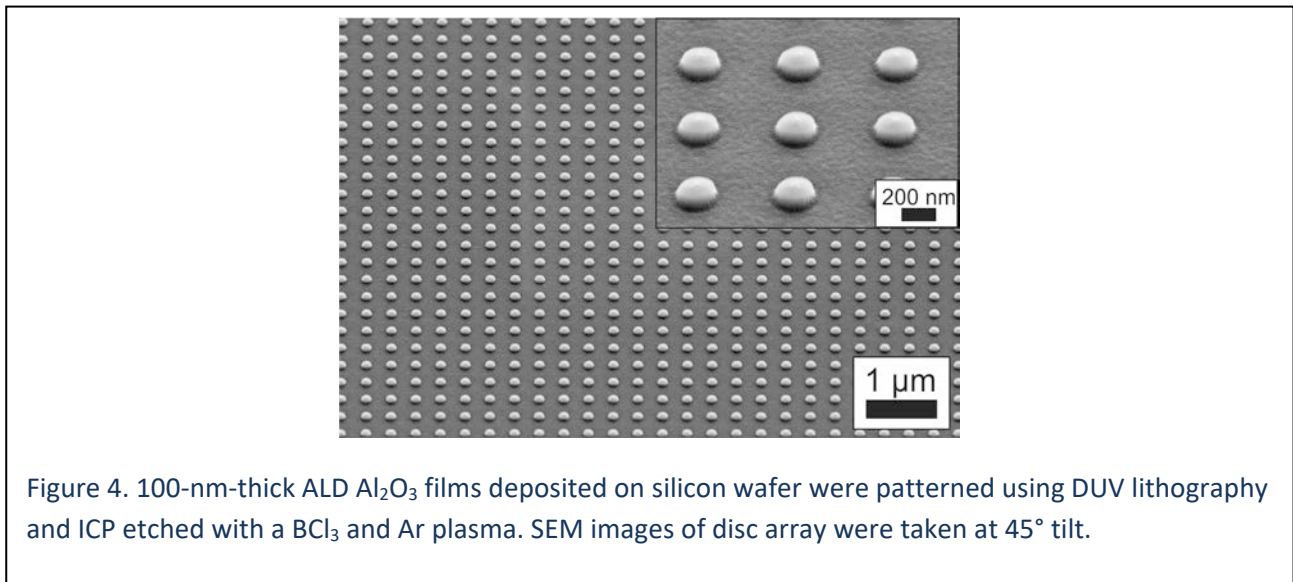


Figure 3. Etch selectivity of DUV resist over alumina and alumina etch profile angle with substrate bias varying between 10 and 100 W. The DUV resist was not removed before sample cleaving and SEM. The ICP contained 50% BCl₃, and pressure was set to 5 mTorr.

In this report, we studied the substrate bias power that modulates the kinetic energy of plasma ions. Figure 3 shows the alumina etch profile angle dependency on the substrate bias power. The bias power varied between 10 and 100 W, while the other parameters were kept constant at 50% BCl_3 and 50% Ar and 5 mTorr pressure. The profile angle decreased drastically to 30° as the bias power increased to 100 W. The physical etch dominated as the power increase to 100 W. Resist selectivity expectedly deteriorated, and resist erosion was clearly visible. The etch rate linearly increased fivefold from 0.2 nm/s to 1 nm/s as the bias power increased from 10 to 100W, which agreed well with prior art [11].

Having optimized alumina etching, as a demonstration, we transferred the nanopatterns into the alumina and the silicon substrate. Using DUV lithography, we patterned gratings, disc arrays, and cavity arrays down to 200 nm and 400 nm pitch. The patterns were then transferred into a 100-nm-thick ALD Al_2O_3 layer and subsequently into the underlying silicon wafer. Figure 4 show SEM images of ALD alumina disc arrays on the exposed underlying silicon substrate. For even smaller patterns we used EBL.



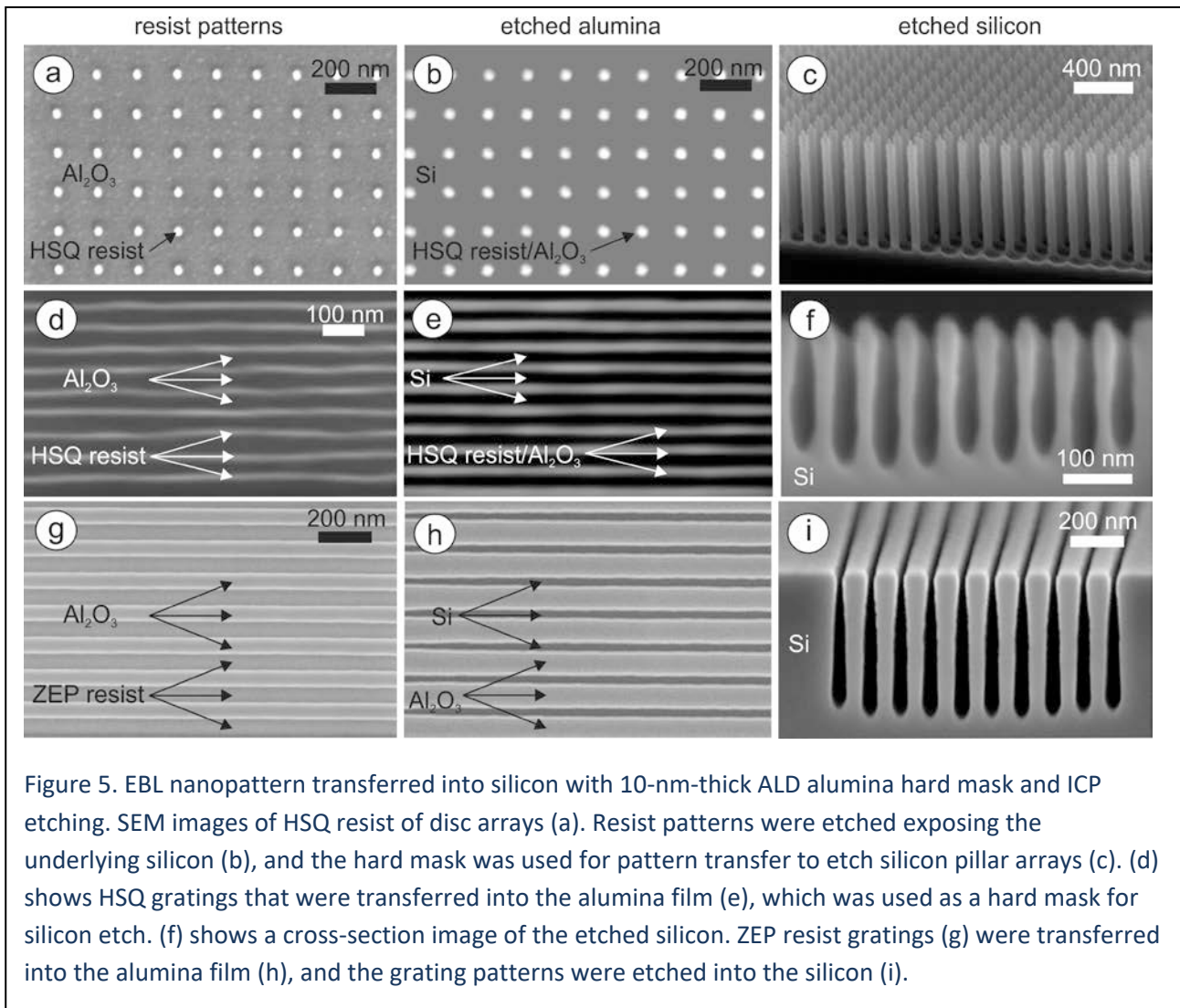
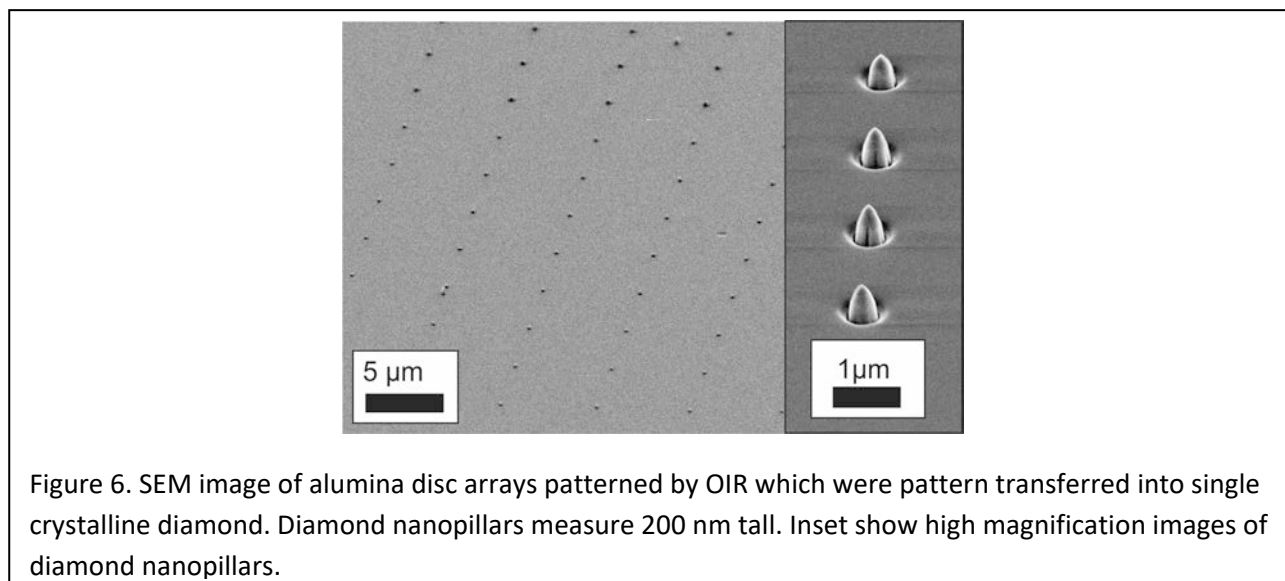


Figure 5. EBL nanopattern transferred into silicon with 10-nm-thick ALD alumina hard mask and ICP etching. SEM images of HSQ resist of disc arrays (a). Resist patterns were etched exposing the underlying silicon (b), and the hard mask was used for pattern transfer to etch silicon pillar arrays (c). (d) shows HSQ gratings that were transferred into the alumina film (e), which was used as a hard mask for silicon etch. (f) shows a cross-section image of the etched silicon. ZEP resist gratings (g) were transferred into the alumina film (h), and the grating patterns were etched into the silicon (i).

For EBL patterning, we used the negative tone HSQ resist and the positive tone ZEP resist (Fig. 5). With 40-nm-thick HSQ, we patterned gratings, and disc arrays. The HSQ discs were 30 nm in diameter and the array pitch was 150 nm. The patterns were transferred by ICP etch into the 10-nm-thick ALD alumina and the disc diameter increased slightly to 40 nm. The HSQ/alumina hard mask was used for ICP etch of silicon. We obtained vertical side wall Si pillar arrays 56 nm in diameter and 770 nm tall using a standard and non-optimized process. For HSQ gratings, the finest lines were 14 nm, and the pitch was 50 nm. The lines broadened slightly to 18 nm after pattern transfer into alumina, and using it as the hard mask, we etched 180 nm into the silicon. Using 80-nm-thick ZEP, we patterned gratings and cavity arrays. The finest gratings had 40 nm line-width and 120 nm pitch. Resist patterns were transferred into the alumina with ICP etching. The remaining ZEP was removed, and the anticipated narrower alumina lines were subsequently used as a hard mask for silicon etching. The etch depth was 300 nm and the aspect ratio was measured to 7.5. For both HSQ and ZEP, the patterned gratings had a slightly negative etch profile. This was possibly due to charging effects of non-conductive HSQ and alumina hard mask, which deflects the incoming ion species during Si plasma etching, and thus give a negative etching profile.

[26], chromium [27], and ALD alumina assisted pattern transfer of directed self-assembly (DSA) of block copolymers [17], [18]. Aspect ratios higher than 50 for sub-50 nm structures was reported [24], [25]. Prior art and our research shows that alumina can be a promising mask for nanoscale high aspect ratio etching.



In the second demonstration using ALD alumina as hard etch mask, the alumina patterns were transferred into single crystalline diamond (Figure 6). The lithography was performed using organic ice resist method [21]. The alumina mask is just 10-nm-thick, and it enables 200 nm deep etch into diamond. The masking alumina disc diameter is 200 nm, and diamond nanopillar is 200 nm tall, and its base is 400 nm in diameter. The diamond ICP process under-etched the alumina mask, which resulted in a tip shape.

Conclusions

We investigated ICP etching of ALD alumina on the nanoscale, and we provide a process development guideline. To avoid redeposition, an oxygen plasma chamber conditioning step is required before alumina etching. The resist is etched slightly faster than alumina, which means significant mask erosion that is transferred into the etch profile. For etching thicker alumina films, we recommend 2 mTorr, 25% Ar, 75% BCl₃. A 5 mTorr and 50% BCl₃ plasma is more robust in terms of plasma stability and resist selectivity, but it has an inferior etch profile. Unfortunately, both plasmas will lead to redeposition when etching the underlying silicon layer. For thinner alumina films and breaking through to underlying silicon, we recommend 10 mTorr, 100% BCl₃ plasma, but this process will quickly erode the resist mask. If trace amounts of alumina can be tolerated and resist erosion must be kept at a minimum, we recommend a 50% BCl₃ plasma at 10 mTorr. We recommend the lowest possible substrate bias for anisotropic etch, and high bias for low profile angle. For future studies, because prior work and we observed the best etching conditions at low pressures, we recommend the exploration of even lower pressure regimes, for example using an electron cyclotron resonance plasma etching or reactive ion beam etching.

Acknowledgement

We thank the DTU Danchip staff for instrument support. Especially, we thank Ms. Berit Herstrøm, Mr. Jonas Michael-Lindhard, and Dr. Rasmussen for fruitful discussions.

References

- [1] M. D. Henry, S. Walavalkar, a Homyk, and a Scherer, "Alumina etch masks for fabrication of high-aspect-ratio silicon micropillars and nanopillars.," *Nanotechnology*, vol. 20, no. 25, p. 255305, 2009.
- [2] J. Dekker, K. Kolari, and R. Puurunen, "Inductively coupled plasma etching of amorphous Al₂O₃ and TiO₂ mask layers grown by atomic layer deposition," *J. Vac. Sci. Technol. B*, vol. 24, pp. 2350–2355, 2006.
- [3] S. Tegen, "Etch Characteristics of Al₂O₃ in ICP and MERIE plasma etchers," *J. Electrochem. Soc.*, vol. 152, no. 4, 2005.
- [4] T. M. Babinec, B. J. M. Hausmann, M. Khan, Y. Zhang, J. R. Maze, P. R. Hemmer, and M. Loncar, "A diamond nanowire single-photon source," *Nat. Nanotechnol.*, vol. 5, no. 3, pp. 195–199, 2010.
- [5] B. J. M. Hausmann, M. Khan, Y. Zhang, T. M. Babinec, K. Martinick, M. McCutcheon, P. R. Hemmer, and M. Loncar, "Fabrication of diamond nanowires for quantum information processing applications," *Diam. Relat. Mater.*, vol. 19, no. 5–6, pp. 621–629, 2010.
- [6] K.-R. Choi, J.-C. Woo, Y.-H. Joo, Y.-S. Chun, and C.-I. Kim, "Dry etching properties of TiO₂ thin films in O₂/CF₄/Ar plasma," *Vacuum*, vol. 92, pp. 85–89, 2013.
- [7] D.-P. Kim, G.-H. Kim, J.-C. Woo, D.-S. Um, and C.-I. Kim, "The Etching Properties of Al₂O₃ Thin Films in BCl₃/Cl₂/Ar Plasma," *Ferroelectrics*, vol. 384, no. 1, pp. 39–46, Jun. 2009.
- [8] S.-M. Koo, D.-P. Kim, K.-T. Kim, and C.-I. Kim, "The etching properties of Al₂O₃ thin films in N₂/Cl₂/BCl₃ and Ar/Cl₂/BCl₃ gas chemistry," *Mater. Sci. Eng. B*, vol. 118, no. 1–3, pp. 201–204, 2005.
- [9] X. Yang, J. Woo, D. Um, and C. Kim, "Dry Etching of Al₂O₃ Thin Films in O₂/BCl₃/Ar Inductively Coupled Plasma," *Trans. Electr. Electron. Mater.*, vol. 11, no. 5, pp. 202–205, 2010.
- [10] X. Yang, J. Woo, D. Um, and C. Kim, "Dry Etching of Al₂O₃ Coupled Plasma Thin Films in O₂/BCl₃/Ar Inductively Coupled Plasma," *Transactions on Electrical and Electronic Materials*, vol. 11, no. 5, pp. 202–205, 2010.
- [11] X. Yang, D.-P. Kim, D.-S. Um, G.-H. Kim, and C.-I. Kim, "Temperature dependence on dry etching of Al₂O₃ thin films in BCl₃/Cl₂/Ar plasma," *J. Vac. Sci. Technol. A Vacuum, Surfaces, Film.*, vol. 27, no. 4, p. 821, 2009.
- [12] D.-P. Kim, J.-W. Yeo, and C.-I. Kim, "Etching properties of Al₂O₃ films in inductively coupled plasma," *Thin Solid Films*, vol. 459, no. 1–2, pp. 122–126, Jul. 2004.
- [13] Y. P. Hsu, S. J. Chang, Y. K. Su, J. K. Sheu, C. H. Kuo, C. S. Chang, and S. C. Shei, "ICP etching of sapphire substrates," *Opt. Mater. (Amst.)*, vol. 27, no. 6, pp. 1171–1174, 2005.
- [14] D. J. Kang, I. S. Kim, J. H. Moon, and B. T. Lee, "Inductively coupled plasma reactive ion etching of sapphire using C₂F₆- and NF₃-based gas mixtures," *Mater. Sci. Semicond. Process.*, vol. 11, no. 1, pp. 16–19, 2008.

- [15] K. Rasmussen, "Advanced dry etching studies for micro- and nano-systems," 2014.
- [16] X. Wang and M. Goryll, "Nanopore patterning using Al₂O₃ hard masks on SOI substrates," *J. Micromechanics Microengineering*, vol. 25, no. 7, p. 75020, Jul. 2015.
- [17] H. S. Moon, J. Y. Kim, H. M. Jin, W. J. Lee, H. J. Choi, J. H. Mun, Y. J. Choi, S. K. Cha, S. H. Kwon, and S. O. Kim, "Atomic layer deposition assisted pattern multiplication of block copolymer lithography for 5 nm scale nanopatterning," *Adv. Funct. Mater.*, vol. 24, no. 27, pp. 4343–4348, 2014.
- [18] W. Chen, J. Luo, L. Meng, J. Li, J. Xiang, J. Li, W. Wang, D. Chen, T. Ye, and C. Zhao, "Atomic layer deposition assisted pattern transfer technology for ultra-thin block copolymer films," *Thin Solid Films*, vol. 613, pp. 32–37, 2016.
- [19] T. Greibe, T. A. Anhøj, L. S. Johansen, and A. Han, "Quality control of JEOL JBX-9500FSZ e-beam lithography system in a multi-user laboratory," *Microelectron. Eng.*, vol. 155, pp. 25–28, Apr. 2016.
- [20] E. Shkondin, O. Takayama, J. M. Lindhard, P. V. Larsen, M. D. Mar, F. Jensen, and A. V. Lavrinenko, "Fabrication of high aspect ratio TiO₂ and Al₂O₃ nanogratings by atomic layer deposition," *J. Vac. Sci. Technol. A Vacuum, Surfaces, Film.*, vol. 34, no. 3, p. 31605, May 2016.
- [21] W. Tiddi, H. T. Le, M. Beleggia, and A. Han, "Organic Ice Resists," *Under Rev.*
- [22] T. J. Dalton, "Microtrench Formation in Polysilicon Plasma Etching over Thin Gate Oxide," *J. Electrochem. Soc.*, vol. 140, no. 8, p. 2395, 1993.
- [23] J. C. Arnold and H. H. Sawin, "Charging of pattern features during plasma etching," *J. Appl. Phys.*, vol. 70, no. 10, p. 5314, 1991.
- [24] K. J. Morton, G. Nieberg, S. Bai, and S. Y. Chou, "Wafer-scale patterning of sub-40 nm diameter and high aspect ratio (50:1) silicon pillar arrays by nanoimprint and etching," *Nanotechnology*, vol. 19, no. 34, p. 345301, Aug. 2008.
- [25] M. M. Mirza, H. Zhou, P. Velha, X. Li, K. E. Docherty, A. Samarelli, G. Ternent, and D. J. Paul, "Nanofabrication of high aspect ratio (~50:1) sub-10 nm silicon nanowires using inductively coupled plasma etching," *J. Vac. Sci. Technol. B Microelectron. Nanom. Struct.*, vol. 30, no. 6, p. 06FF02, 2012.
- [26] J. Chai, G. Walker, L. Wang, D. Massoubre, S. H. Tan, K. Chaik, L. Hold, and A. Iacopi, "Silicon etching using only Oxygen at high temperature: An alternative approach to Si micro-machining on 150 mm Si wafers," *Sci. Rep.*, vol. 5, p. 17811, Dec. 2015.
- [27] L. A. Woldering, R. Willem Tjerkstra, H. V Jansen, I. D. Setija, and W. L. Vos, "Periodic arrays of deep nanopores made in silicon with reactive ion etching and deep UV lithography," *Nanotechnology*, vol. 19, no. 14, p. 145304, Apr. 2008.

Referees

Dr. Boon Teik Chan, plasma etching, IMEC Belgium. E-mail: bt.chan@imec.be

Prof. Dr. Sami Franssila, ALD and plasma etching, Alto University, Finland. E-mail: sami.franssila@alto.fi

Prof. Dr. Zheyao Wang, plasma etching of silicon, Tsinghua University, China. E-mail: z.wang@tsinghua.edu.cn